due to the Jahn-Teller effect. The frequency dependence of the loss shows that it is a relaxation rather than a resonant process. While there is some deviation from the theoretical dependence at the lowest frequencies it is not in the direction expected for a resonant process. This result is consistent with the presence of small random strains in the crystal, which broaden the resonance and localize the wave functions sufficiently that a relaxation calculation is valid.

From our data we have deduced a temperature dependent relaxation time which is in good agreement with the relaxation time deduced from the transition from the static to dynamic Jahn-Teller effect observed in spin resonance. At relatively high temperatures the relaxation time shows the usual thermal activation type of behavior, but at low temperatures effects of tunneling are seen. We conclude from the temperature dependence below 6°K that tunneling accompanied by one-phonon emission is the primary relaxation process.

ACKNOWLEDGMENTS

We are grateful to Dr. P. Gosar and Dr. J. A. Sussman for preprints and for helpful and stimulating correspondence, and to M. B. Graifman for help with the spin-resonance experiment.

PHYSICAL REVIEW VOLUME 155, NUMBER 2 10 MARCH 1967

Magnetic Relaxation in Nickel above the Curie Temperature*

M. B. SALAMON†
Department of Physics, University of California, Berkeley, California
(Received 8 August 1966; revised manuscript received 9 November 1966)

Magnetic relaxation in nickel above the Curie temperature (354°C) has been studied up to a temperature of 450°C. The spin-relaxation rate $1/\tau_r$, which is equal to the magnetic resonance half-width $\Delta\omega=\gamma\Delta H$, is determined from the field dependence of the microwave Kerr rotation. We fit the relaxation to an expression: $1/\tau_r=3(C/T)(H/M)\omega_d^2\tau_c$, where C is the Curie constant, T the absolute temperature, M/H the transverse static susceptibility, ω_d the pseudodipolar coupling frequency, and τ_c the spin correlation time. At high temperatures, τ_c is constant and is set equal to $1/\omega_e$, the reciprocal exchange frequency, by a suitable choice of ω_d. As the temperature is dropped below 420°C, τ_c begins to increase as $(T-T_c)^{-2/3}$. This increase in τ_c is compatible with critical-neutron-scattering studies of nickel and with measurements of the static susceptibility. Below 385°K, τ_c remains constant at a value 1.8 times the high-temperature value. It is believed that the development of spin-wave excitations in this temperature range prevents a further increase in the spin correlation time. A shift in the spectroscopic splitting factor from $g=2.22$ below T_c to $g=2.29$ above T_c is observed. Well above T_c, a small amount of Kerr rotation, which is associated with the Hall effect, is observed. The magnitude of this rotation is consistent with the results of dc studies.

I. INTRODUCTION

RECENTLY, the magnetic critical point has been the subject of considerable theoretical and experimental investigation. Approximate solutions for the Ising and Heisenberg models have given accurate expressions for the transition temperature[1] and the initial susceptibility in the critical region. For a face-centered cubic lattice and spin $\frac{1}{2}$ the initial susceptibility is found for both models to be of the form

$$\chi_0 \propto (T-T_c)^{-\gamma}. \quad (1)$$

The exponent γ is 5/4 for the Ising model[2] and 4/3 for the Heisenberg model[3] for all three-dimensional lattices. The deviation from the Curie-Weiss value $\gamma=1$ is the result of short-range correlations which are neglected in a molecular-field calculation but which have been examined in more recent work.

Kouvel and Fisher[4] have re-examined the magnetization data of Weiss and Forrer[5] for nickel and find that, near T_c,

$$\gamma_{\mathrm{Ni}}=1.35\pm0.02. \quad (2)$$

Recent measurements by Arajs[6] confirm this result. Similarly, the value of γ for iron[6,7] has been found to be 1.33 ± 0.04. These results indicate that correlation effects play an important role in these metals and that the Heisenberg model appears to give an adequate description of their behavior.

* Supported by the U. S. Atomic Energy Commission through Contract No. AT(11-1)-34, Project 47. Report Code No. UCB-34P47-3.

† National Science Foundation Cooperative Fellow, 1963–1965. Present address: Department of Physics, University of Illinois, Urbana, Illinois.

[1] C. Domb and A. R. Miedema, in *Progress in Low Temperature Physics*, edited by C. J. Gorter (North-Holland Publishing Company, Amsterdam, 1964), pp. 297–343.

[2] C. Domb and M. F. Sykes, J. Math. Phys. **2**, 63 (1961); G. A. Baker, Phys. Rev. **124**, 768 (1961).

[3] C. Domb and M. F. Sykes, Phys. Rev. **128**, 168 (1962); G. A. Baker, *ibid.* **129**, 99 (1963).

[4] J. S. Kouvel and M. E. Fisher, Phys. Rev. **136**, A1626 (1964).

[5] P. Weiss and R. Forrer, Ann. Phys. (Paris) **5**, 153 (1926).

[6] S. Arajs, J. Appl. Phys. **36**, 1136 (1965).

[7] J. E. Noakes and A. Arrott, J. Appl. Phys. **35**, 931 (1964).

Neutron-diffraction measurements[8] have shown clearly the importance of short-range order in the understanding of the critical region. By making an analogy with critical opalescence at the liquid-gas critical point, Van Hove[9] was able to interpret the neutron data near T_c within the Ornstein-Zernike theory of critical fluctuations. The close relation between the magnetic transition and the liquid-gas critical point has been developed further by several authors.[10] The important result is that large-scale fluctuations of the local magnetization occur near the transition temperature, with spins becoming correlated over increasingly longer distances, and for longer times, as the transition temperature is approached from above.

With such large-scale activity in the spin system, one might expect anomalous behavior in the resonance properties of magnetic materials near their transition temperatures. A divergence of both the electronic[11] and nuclear[12] resonance linewidths in MnF_2 at the Néel temperature has been observed and attributed to critical fluctuations[13]. An increase in the linewidth in iron[14] and nickel[15,16] has also been found in the transition region. We have made a detailed measurement of the linewidth in nickel from the Curie point[4] ($T_c=627$°K) to 723°K finding that the linewidth increases rapidly with an anomaly occurring 30°K *above* the Curie point. The increasing half-width was measured up to 13 kOe; the predicted[17] high-temperature half-width, due to exchange narrowing of the pseudo-dipolar interaction, is 120 kOe.

Because of the large measured linewidths, ordinary resonance techniques could not be employed. Sufficient sensitivity for broad lines was obtained with the use of a bimodal cavity superheterodyne spectrometer.[18] This spectrometer, because of its frequency-independent balance, permits the measurement of very small changes in the polarization of the rf field in the cavity.

In the simple case of a single reflection from an isotropic metal surface, the circularly polarized components of a normally incident wave are reflected independently. If the sample is made anisotropic, for instance by the application of a magnetic field, the indices of refraction $N^{\pm}$ for the rotating components will be different, and the reflected wave will have its polarization direction rotated by an angle,

$$\varphi=(N^{+}-N^{-})/(N^{+}N^{-}-1), \tag{3}$$

with respect to the plane-polarized incident wave. When the rotation is due to the difference in the rotating permeabilities $\mu^{\pm}=1+4\pi\chi^{\pm}$, it is called the Kerr effect, and the angle is given by

$$\begin{aligned}\varphi&\cong(1-i)(\delta/\lambda)[(\mu^{+})^{1/2}-(\mu^{-})^{1/2}]\\&\cong 2\pi(1-i)(\delta/\lambda)(\chi^{+}-\chi^{-})\end{aligned} \tag{4}$$

for $4\pi\chi^{\pm}\ll 1$. Here $\chi^{\pm}$ are the rotating susceptibilities, δ is the skin depth, and λ is the wavelength in the cavity. Near resonance, the rotation angle becomes

$$\mathrm{Re}\,\varphi\cong(\delta/\lambda)\chi_0(H/\Delta H), \tag{5}$$

where χ_0 is the static susceptibility, H is the field for resonance, and ΔH is the linewidth. For $\delta\approx 10^{-4}$ cm, $\chi_0\approx 10^{-3}$, and $\Delta H\approx 10^{5}$ Oe we obtain a rotation angle of 10^{-8} rad/reflection for K-band frequencies. If we place the sample in a cavity which has two orthogonal modes resonant at the same frequency we can determine the rotation angle by measuring the power coupled by the sample from the excited mode to the decoupled mode. The rotation will be enhanced by the Q of the cavity. For the bimodal cavity used in this experiment a rotation of 10^{-8} rad/reflection changes the power in the decoupled mode by 10^{-12} W, which is the limit of detection for our spectrometer. In practice rotations were larger than 10^{-7} rad and the resulting 10^{-11} W change in the coupled power was easily detected.

II. EXPERIMENT

A longitudinal section of the bimodal cavity, resonant in the TE_{111} mode at 23.34 GHz, is shown in Fig. 1.[18] Incident microwave power excites the cavity through the coupling iris in one end wall. By means of the resistive and capacitative tuning plugs shown in Fig. 2, the cavity can be balanced so that no microwave power is transmitted into the second waveguide; isolation of the second waveguide by 80 dB can be attained

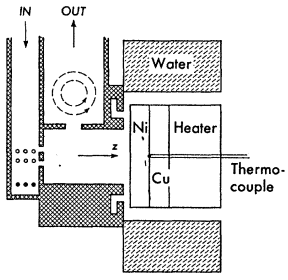

FIG. 1. A longitudinal section of the bimodal cavity. A vane placed in the iris in the left end-wall varies the coupling into the two modes. Power coupled into the top waveguide goes to the balanced mixer.

[8] C. G. Shull and M. K. Wilkenson, Phys. Rev. **103**, 516 (1956).
[9] L. Van Hove, Phys. Rev. **95**, 1374 (1954).
[10] D. S. Gaunt, M. E. Fisher, M. F. Sykes, and J. W. Essam, Phys. Rev. Letters **13**, 713 (1964); G. B. Benedek, in Conference on Phenomena in the Neighborhood of Critical Points, National Bureau of Standards, Washington, D. C., April 1965 (to be published).
[11] F. M. Johnson and A. H. Nethercott, Jr., Phys. Rev. **114**, 705 (1959); J. C. Burghiel and M. W. P. Strandberg, J. Appl. Phys. **35**, 852 (1964).
[12] P. Heller and G. B. Benedek, Phys. Rev. Letters **8**, 428 (1962).
[13] T. Moriya, Progr. Theoret. Phys. (Kyoto) **28**, 371 (1962).
[14] D. S. Rodbell, in *Growth and Perfection in Crystals* (John Wiley & Sons, Inc., New York, 1958), p. 247.
[15] N. Bloembergen, Phys. Rev. **78**, 572 (1950).
[16] D. S. Rodbell, Phys. Rev. Letters **13**, 471 (1964); in *Proceedings of the International Conference on Magnetism, Nottingham, 1964* (The Institute of Physics and The Physical Society, London, 1965), p. 227; Physics **1**, 279 (1965).
[17] B. R. Cooper and F. Keffer, Phys. Rev. **125**, 896 (1962).
[18] A. M. Portis and Dale Teaney, J. Appl. Phys. **29**, 1692 (1958); Dale T. Teaney, M. P. Klein, and A. M. Portis, Rev. Sci. Instr. **32**, 721 (1961).

by careful tuning. To adjust the coupling of the two modes, a small metal vane is placed in the input iris. With this final adjustment it is possible to achieve a frequency-independent balance over the full cavity resonance.

Rotation of the polarization of the microwave fields by the sample causes power to be coupled into the second waveguide. Since the sample will be both lossy and dispersive, the reflected wave will become elliptically polarized as indicated by Eq. (4). By perturbing the cavity either capacitatively (with a capacitative plug) or resistively (with a resistive plug) the rotation angle or the ellipticity, respectively, can be measured.

As shown in Fig. 1, the nickel sample, mounted in a copper holder, forms one end wall of the cavity. A small vacuum space provides thermal insulation, allowing the sample to be heated to 500°C while the water-cooled cavity remains at about 15°C. In order that very little microwave power leak into the vacuum space, a choke joint was constructed to reflect a short at the cavity-sample boundary. A small inconel spacer keeps the sample a fixed distance from the end wall of the cavity and parallel to it. No change in cavity frequency was found on heating the sample from room temperature 500°C so that a signal from mechanical sources can be safely assumed to be negligible.

In order to detect the small in power ($\sim 10^{-11}$ W) which result from the Kerr rotation, a superheterodyne detector, a block diagram of which is shown in Fig. 3, is used. To avoid having to stabilize the local oscillator (LO) at the 60 MHz difference frequency, the frequency of the LO is swept through twice the bandwidth of the IF amplifier. In this way drifts of several megacycles in LO frequency cause no change in the signal amplitude. The signal klystron is stabilized at the cavity frequency by means of an AFC system.

Because only the sample is heated, a fast, sensitive temperature-control system is necessary. With a thermistor used as the resistive element in an ac bridge, a satisfactory system was constructed using a phase-sensitive detector to drive both a transistor current amplifier and a servo-motor in the power supply. This system is capable of controlling the sample temperature to ± 0.01°C for short periods and to ± 0.1°C for several hours. A block diagram is inset in Fig. 3. The actual temperature of the sample is measured with a Pt–Pt+10% Rh thermocouple placed in good thermal contact with the sample.

Two single-crystal nickel samples were used in this experiment. Each was spark-cut into a disk from a single-crystal ingot, lightly hand polished to remove the spark pits, and then annealed in vacuum for 2h at 1000°C. Care was taken to cool the samples slowly to avoid straining. X-ray diffraction plates taken after annealing showed that the samples were single crystals and were unstrained. Sample I was cut along a {110} plane from an ingot analyzed as 99.995% pure. After being annealed, it was soldered to a copper back and electropolished to its final size: 16 mm in diameter by 1.6 mm thick. Sample II was cut along a {100} plane from a different ingot of much greater purity—fewer than 40 ppm total impurity. To eliminate a possible source of strain, the copper back was electro-formed directly onto the sample which was waxed to an aluminum mandrel. After the aluminum was dissolved away, the sample was electropolished to 13 mm in diameter by 1.3 mm thick. The samples are heated by a small heater in good thermal contact with the copper back. All mountings and connections are made to the copper, so that a constant temperature is maintained throughout the sample.

III. ANALYSIS OF ROTATION

The analysis of the bimodal cavity is greatly simplified by the introduction of lumped circuit elements.[18] In the equivalent circuit the effect of the sample is contained in a sample-impedance tensor $\mathbf{z}=\mathbf{r}+i\mathbf{x}$ which perturbs the cavity. For capacitative unbalance, the fractional change in coupled power P_2 in the second waveguide was calculated to be[18]

$$\left(\frac{\delta P_2}{P_2}\right)_C \cong \frac{\cot\theta}{[(1+\beta_1)(1+\beta_2)]^{1/2}}\left(\frac{x_{xx}-x_{yy}}{R}+\frac{x_{xy}-x_{yx}}{R}\right) - \cos^2\theta\left(\frac{1}{1+\beta_1}+\frac{1}{1+\beta_2}\right)\frac{r_{xx}+r_{yy}}{R} - \cos^2\theta\left(\frac{1}{1+\beta_1}+\frac{1}{1+\beta_2}\right)\frac{r_{xy}-r_{yx}}{R} - \sin 2\theta\left(\frac{1}{[(1+\beta_1)(1+\beta_2)]^{1/2}}\right)\frac{x_{xx}-x_{yy}}{R}, \quad (6)$$

where β_1 and β_2 are the coupling constants for the input and output irises, respectively. R is the cavity loss, and $\sin^2 2\theta$ is the ratio of the coupled power to the maximum coupled power.

For resistive unbalance, the fractional change in coupled power is

$$\left(\frac{\delta P_2}{P_2}\right)_R \cong \frac{1/\theta}{[(1+\beta_1)(1+\beta_2)]^{1/2}}\left(\frac{r_{xx}-r_{yy}}{R}+\frac{r_{xy}-r_{yx}}{R}\right) - \left(\frac{1}{1+\beta_1}+\frac{1}{1+\beta_2}\right)\frac{r_{xx}+r_{yy}}{R} - \left(\frac{1}{1+\beta_1}+\frac{1}{1+\beta_2}\right)\frac{r_{xy}+r_{yx}}{R}. \quad (7)$$

In both Eqs. (6) and (7) the first term represents the rotation due to sample anisotropy. The remaining terms represent changes in the microwave power level in the cavity and are comparatively small for small θ.

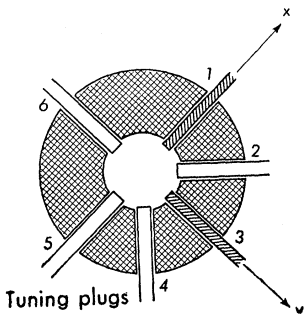

FIG. 2. A transverse section of the bimodal cavity. The shaded tuning plugs are resistive, the remainder, capacitative.

The lumped circuit impedance $\mathbf{z}$ can be easily shown[19] to be related to the surface-impedance tensor $\mathbf{Z}$ through

$$\mathbf{z}/R=(\lambda/\delta)(Qf)\mathbf{Z}, \tag{8}$$

where Q is the cavity Q and f is the sample filling factor. Since it is required by symmetry that $Z_{xx}=Z_{yy}$ and $Z_{xy}=-Z_{yx}$, the only significant terms in (6) and (7) for small θ arise from the term

$$(z_{xy}-z_{yx})/R=(\lambda/\delta)(Qf)(Z_{xy}-Z_{yx}) \tag{9}$$

in the rotation expressions.

The required elements of the surface-impedance tensor for a ferromagnetic metal have been calculated by Young and Uehling.[20] We have extended their calculation by using the Bloch equation as modified by Wangsness[21] for relaxation to the instantaneous field and including the Hall effect.[22] It is necessary to use the Wangsness form since the relaxation occurs in times comparable to a period of the rf field. We find that

$$Z_{xy}-Z_{yx}=(1+i)(\delta/2\lambda)[(\sigma_0\mu^+/\sigma^+)^{1/2}-(\sigma_0\mu^-/\sigma^-)^{1/2}], \tag{10}$$

where σ_0 is the zero-field conductivity, the $\sigma^\pm$ are given

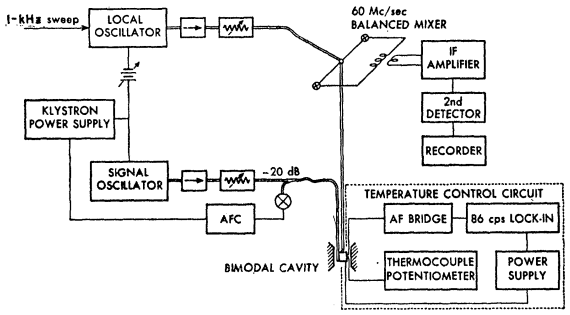

FIG. 3. A block diagram of the bimodal cavity superheterodyne spectrometer and the temperature control circuit. AFC stands for automatic frequency control, AF for audio frequency, and IF for intermediate frequency.

by

$$\sigma^\pm=\sigma_0(1\pm i\theta_H), \tag{11}$$

and θ_H is the Hall angle for an applied field H. The rotating permeabilities are easily shown[19] to be given by

$$\mu^\pm=1+4\pi(\chi_1^\pm+i\chi_2^\pm),$$

where

$$\chi_1^\pm=\chi_0\left\{1-\frac{(\omega-\omega_0)\omega\tau_r^2}{[1+(\omega\pm\omega_0)^2\tau_r^2]}\right\}, \tag{12}$$

$$\chi_2^\pm=\chi_0\left\{\frac{\omega\tau_r}{[1+(\omega\pm\omega_0)^2\tau_r^2]}\right\}, \tag{13}$$

and where $\omega_0=\gamma(H_0-N_zM)$ and τ_r is the single relaxation parameter in the Wangsness equation. Assuming the sample to be an ellipsoid with an axial ratio of 10, we find that the demagnetizing factor N_z is 10.97.[23]

The separation of (10) into real and imaginary parts is shown in Ref. (20). However, when the static susceptibility and Hall angle are small, the rotation expressions can be expanded to give on capacitative unbalance

$$\left(\frac{\delta P_2}{P_2}\right)_C\cong\frac{(1/\theta)Qf}{[(1+\beta_1)(1+\beta_2)]^{1/2}}\times\{\pi[(\chi_1^+-\chi_1^-)+(\chi_2^+-\chi_2^-)]-\theta_H/2\} \tag{14}$$

and on resistive unbalance

$$\left(\frac{\delta P_2}{P_2}\right)_R\cong\frac{(1/\theta)Qf}{[(1+\beta_1)(1+\beta_2)]^{1/2}}\times\{\pi[(\chi_1^+-\chi_1^-)-(\chi_2^+-\chi_2^-)]-\theta_H/2\}. \tag{15}$$

The mixture of dispersive and absorptive components in Eqs. (14) and (15) makes analysis of the data difficult. If, however, data for each unbalance are taken at the same temperature and with the same value of θ, the resultant curves can be added and subtracted to separate the components. That is, we form

$$\left(\frac{\delta P_2}{P_2}\right)_C+\left(\frac{\delta P_2}{P_2}\right)_R=\frac{A}{\theta}[\chi_1^+-\chi_1^-], \tag{16}$$

which is the dispersive part, and

$$\left(\frac{\delta P_2}{P_2}\right)_C-\left(\frac{\delta P_2}{P_2}\right)_R=\frac{A}{\theta}[(\chi_2^+-\chi_2^-)-\theta_H/2\pi], \tag{17}$$

which is the absorptive part. The gain factor A is given by

$$A=2\pi Qf/[(1+\beta_1)(1+\beta_2)]^{1/2}.$$

Because the Hall effect is out of phase with the driving field it appears only in the absorptive term.

[19] M. B. Salamon, thesis, University of California, Berkeley, 1965 (unpublished). Available from University Microfilms, 300 Zeeb Road, Ann Arbor, Michigan.
[20] J. A. Young, Jr., and Edwin A. Uehling, Phys. Rev. **94**, 544 (1953).
[21] R. K. Wangsness, Phys. Rev. **98**, 927 (1955).
[22] P. R. Miller, Phys. Rev. **121**, 435 (1960).
[23] J. A. Osborn, Phys. Rev. **67**, 351 (1945).

Exactly at resonance Eqs. (16) and (17) have the values

$$(\delta P_2/P_2)_C+(\delta P_2/P_2)_R=2A\chi_0\omega^2\tau_r^2/\theta(1+4\omega^2\tau_r^2), \quad (18)$$

and

$$(\delta P_2/P_2)_C-(\delta P_2/P_2)_R =4A\chi_0\omega^3\tau_r^3/\theta(1+4\omega^2\tau_r^2)+A\theta_H/2\pi\theta. \quad (19)$$

We can therefore use the amplitude of the signals as a check on the value of τ_r obtained from the line shape.

In the temperature region where the expansion of (10) is valid, the dispersive and absorptive parts were separated according to Eqs. (16) and (17), and compared with shapes computed on an IBM 1620 computer. Near the transition temperature, a least-squares fit to the rotation expression given in Ref. 20, was made on the computer with two adjustable parameters, τ_r and γ. The least-squares analysis agrees with the line-shape analysis in the region where both could be used.

IV. LINEWIDTH

A. Experimental Results

At each temperature the Kerr rotation was measured on both resistive and capacitative unbalance as a function of applied field. Four sweeps of the field from 0 to 12 kOe were made with each type of unbalance, two with the field in the $+z$ direction and two with the field in the $-z$ direction. The resultant curves were averaged and the best value of τ_r to fit both resistive and capacitative curves was determined by the methods discussed in Sec. III. Typical data are shown in Fig. 4. Values for the magnetization and the susceptibility used in analyzing our data were taken from the work of Weiss and Forrer.[5]

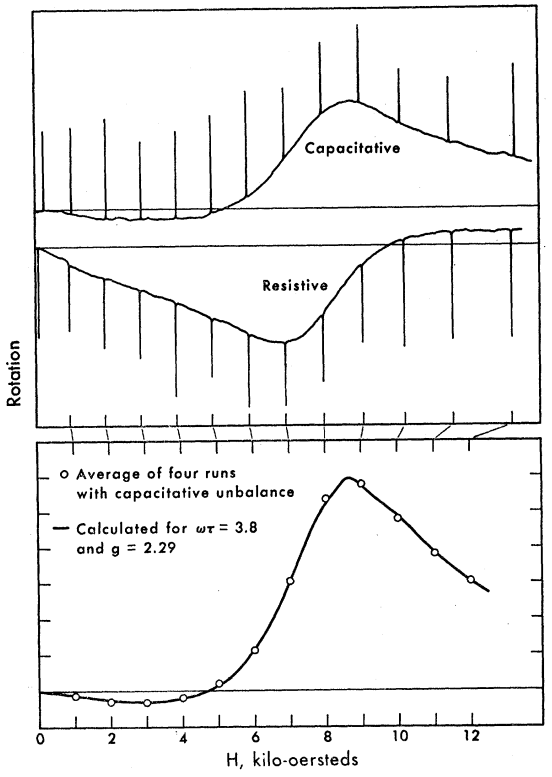

FIG. 4. Recorder traces taken at 362°C (T_c+8°K) with $1/\theta=200$. The circles on the bottom curve are the average of four capacitative sweeps; the calculated curve is for $\omega\tau=3.8$ for which $2\Delta H=3.8$ kOe.

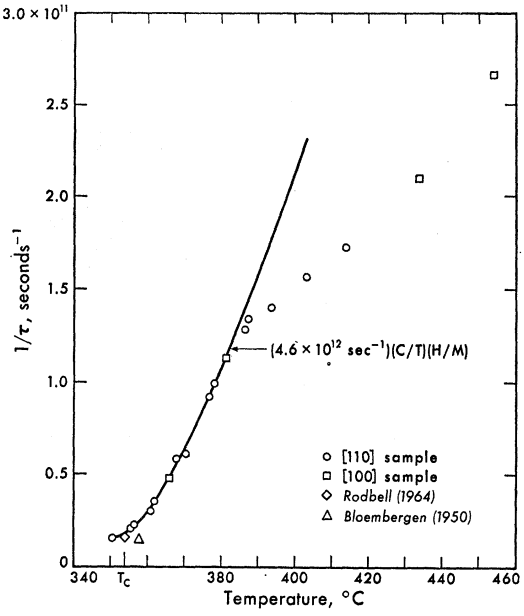

FIG. 5. The relaxation frequency τ_r^{-1} versus temperature. The linewidth corresponding to the highest point is 27 kOe.

Measured values of the relaxation rate $1/\tau_r$ are shown as a function of temperature in Fig. 5. Although the two samples used in this experiment differ in orientation, purity, and the method of mounting as discussed in Sec. III, no differences in their resonance properties could be detected, as seen from Fig. 5. The most rapid relaxation rate measured, 2.7×10^{11} sec^{-1}, corresponds to a full linewidth $2\Delta H=27$ kOe.

As is noted in Sec. III, the amplitude of the rotation can be used as an alternative measure of the relaxation rate $1/\tau_r$. We use this result, rather, as a check that the observed rotation is due to the nickel sample by calculating the static susceptibility χ_0 from Eq. (19) using values of τ_r from Fig. 5. In Fig. 6 we compare these calculated values of χ_0 to the experimental values of Weiss and Forrer.[5] We obtain an excellent fit for $A=0.32$. With $Q=1.5\times10^3$ and $\beta_1=\beta_2=0.7$, this value of A gives a filling factor of $f=6\times10^{-5}$. Since the skin depth is 10^{-4} cm and the cavity wavelength is 1.5 cm, we would expect f to be 7×10^{-5} in good agreement with the measured value.

The solid line in Fig. 5 is the curve

$$\tau_r^{-1}=(4.6\times10^{12}\ \text{sec}^{-1})(C/T)(H/M), \quad (20)$$

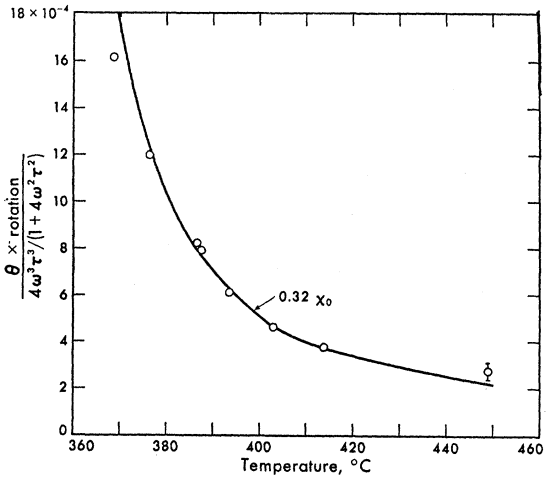

FIG. 6. The static susceptibility χ_0 calculated from the amplitude of the observed Kerr rotation at resonance. The solid line corresponds to 0.32 χ_0 (Ref. 24). The numerical factor 0.32 is the quantity A which occurs in the rotation expressions, Eqs. (18) and (19).

where C is the Curie constant, H is the applied field, and M is the magnetization. Equation (20) has the temperature dependence for the exchange narrowed line predicted by de Gennes *et al.*[24] A simple physical model reproduces this result: We assume that our system of volume V consists of N spins per unit volume, each having a magnetic moment μ and interacting with its nearest neighbors with the pseudodipolar energy D and an exchange energy J. At sufficiently high temperatures, pairs of spins will change their relative orientation randomly at the rate $\omega_e=J/\hbar$. Because each spin precesses at $\omega_d=D/\hbar$ in the pseudodipolar field of its neighbors, the modulation of ω_d due to the thermal flipping of spins at the exchange rate ω_e results in a random walk in orientation with angular steps $\delta\varphi=\omega_d/\omega_e$ taken at the exchange rate. Using the usual random walk argument we find that a spin in a given direction dephases with a mean square angle $\langle\varphi^2\rangle$ which increases as

$$\langle\varphi^2\rangle=n(\delta\varphi)^2=(\omega_d^2/\omega_e)t, \tag{21}$$

where n is the number of steps taken in time t.

If all the spins were initially along the z axis, then at a later time t, a mean-square magnetization

$$\langle M_x^2\rangle=(N\mu^2/V)(\omega_d^2/\omega_e)t \tag{22}$$

would appear in the transverse direction. By the equipartition theorem, (22) has the equilibrium value[25] $\chi_0 k_B T/V$, where the static susceptibility χ_0 is assumed to be isotropic. We therefore regard (22) as the first term of

$$\langle M_x^2\rangle=(k_B T\chi_0/V)[1-\exp(-t/\tau_r)], \tag{23}$$

where the relaxation rate is

$$1/\tau_r=(N\mu^2/k_B T\chi_0)(\omega_d^2/\omega_e). \tag{24}$$

Villain[26] has shown that the ratio M/H should be used for χ_0 near T_c, so that (24) becomes

$$1/\tau_r=(C/T)(H/M)(3\omega_d^2\tau_c), \tag{25}$$

where $C=N\mu^2/3k_B$ is the Curie constant. The same temperature dependence follows from both the Kubo-Tomita theory and a moments calculation of the exchange-narrowed linewidth.[27] In the spirit of the Kubo-Tomita approach, we have written $1/\omega_e=\tau_c$, the spin-spin correlation time.

Referring to Fig. 5 we see that (20) is valid only to about 385°C (T_c+30°K) where an additional temperature dependence appears. From Fig. 7 we see that the data can be interpreted as a shift in the value of $3\omega_d^2\tau_c$ from

$$3\omega_d^2\tau_c=(4.6\pm0.2)\times10^{12}\ \text{sec}^{-1}, \quad \text{for} \quad T-T_c<30°\text{K}$$

to

$$3\omega_d^2\tau_c=(2.5\pm0.5)\times10^{12}\ \text{sec}^{-1}, \text{ for } T-T_c>66°\text{K}. \tag{26}$$

In the intermediate region, the relaxation rate varies as

$$3\omega_d^2\tau_c\propto(T-T_c)^{-\gamma/2}\propto\chi_0^{1/2}, \tag{27}$$

where we have used (1); γ is found to be $\gamma=1.34\pm0.05$ by a least-squares fit.

B. $T-T_c>66°$K: Exchange Narrowing

For temperatures greater than T_c+66°K we hold that the usual assumptions[28] for exchange narrowing are valid and that the observed value $3\omega_d^2\tau_c=(2.5\pm0.5)\times10^{12}$ sec^{-1} is the high-temperature limit of the exchange-narrowed linewidth. In this limit, Cooper and Keffer[17] have calculated the moments of the line using the untruncated Van Vleck Hamiltonian. They find that the linewidth is given by

$$3\omega_d^2\tau_c(T=\infty)=3.07D^2/\hbar J, \tag{28}$$

where D is the nearest-neighbor pseudodipolar coupling constant and J is the exchange constant.

Values of D and J can be determined from the experimental values of the magnetocrystalline anisotropy constants[29] K_1 and K_2 and from the spin-wave dispersion constant, respectively. With $J=5\times10^{-14}$ erg, no single value of D leads to values of both K_1 and K_2 which agree with experiment. Using $K_1(0)=-1.1\times10^6$ erg/cm^3 as given by Puzey[30] we obtain $D/J=0.09$, while Rodbell's[16] value of $K_2(0)\cong-5\times10^5$ erg/cm^3 leads to

[24] P. G. de Gennes, C. Kittel, and A. M. Portis, Phys. Rev. **116**, 327 (1959).
[25] L. D. Landau and E. M. Lifshitz, *Electrodynamics of Continuous Media* (Pergamon Press, Inc., New York, 1965), p. 147.
[26] J. Villain, J. Phys. Radium **24**, 622 (1963).
[27] A. J. Buslik, thesis, University of Pittsburgh, 1962 (unpublished).
[28] P. W. Anderson and P. R. Weiss, Rev. Mod. Phys. **25**, 269 (1953); P. W. Anderson, J. Phys. Soc. Japan **9**, 316 (1954).
[29] R. J. Joenk, Phys. Rev. **130**, 932 (1963).
[30] I. M. Puzey, Fiz. Metal. i Metalloved. **16**, 29 (1963).

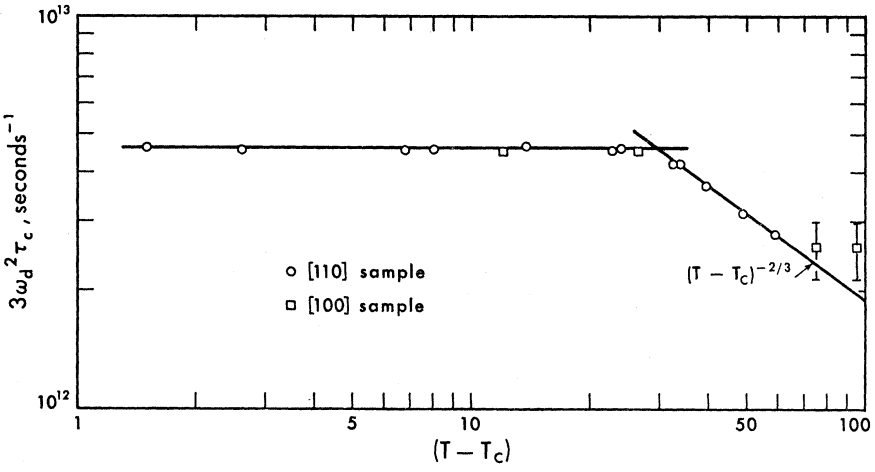

FIG. 7. $3\omega_d^2\tau_c$, as a function of temperature. The error bars shown for the high-temperature points represent the maximum error from all sources.

$D/J=0.19$. With these values of D/J, the Cooper-Keffer linewidth falls in the range

$$1.4\times10^{12}\ \text{sec}^{-1}\leq 3\omega_d^2\tau_c\leq 5.4\times10^{12}\ \text{sec}^{-1} \quad (29)$$

which includes our value of 2.5×10^{12} sec^{-1}. Our results indicate that $D/J=0.13$.

It might be argued that, with somewhat larger error in our highest-temperature points ($+20\%$ instead of $\pm10\%$), they would fall on the $(T-T_c)^{-\gamma/2}$ curve. However the error bars in Fig. 7 are already very generous. We believe that our measurements have carried us into the exchange-narrowing region.

C. $T_c+30°\text{K}\leq T\leq T_c+66°\text{K}$: Critical Fluctuations

Thus far, we have assumed that the rate at which the exchange interaction modulates the pseudodipolar energy is temperature-independent and have considered only the temperature dependence arising from the limited power available to fluctuations. The latter is a macroscopic approximation, taking account only of long-range order (finite magnetization) in the spin system. However, the implications of Eq. (2) and of neutron-scattering experiments[8] lead us to consider the effect of short-range order. Since short-range order implies spin correlation, it will result in a reduction in the average rate at which spin flips occur, and hence, from Eq. (25), in an increase in the apparent high-temperature linewidth.[31]

Neutron-scattering results indicate that in the region immediately above the critical temperature, a magnetic crystal can be thought of as being instantaneously multidomained with domains (clusters) of average radius r_c. The spins within a cluster are aligned, so that only those spins on the surface can make transitions which interrupt the dipole precession. Since only a fraction r_c^2/r_c^3 of the spins are effective, the correlation time τ_c is proportional to the cluster radius r_c. Van Hove has shown[9] that $r_c\propto\chi_0^{1/2}$ in the critical region so that (27) follows if ω_d is temperature-independent.

We now assume that there is a distribution of cluster sizes $P(q)$ with lifetimes $\tau(q)$, where q is the wave vector of the fluctuation. Then a typical spin has a probability $P(q)$ of being in a cluster of radius q^{-1} and therefore relaxing in a time $\tau(q)$. The average relaxation time τ_c is then

$$\tau_c=\textstyle\sum_q P(q)\tau(q). \quad (30)$$

One of the central results of Van Hove's analysis of these fluctuations is that the spatial correlation function γ_r has the form

$$\gamma_r=(4\pi AVr)^{-1}\exp[-r(A\chi_0)^{-1/2}], \quad (31)$$

where A is a parameter associated with the exchange stiffness of the sample. Using this correlation function in the Wiener-Khintchin theorem[32] we obtain the power spectrum $w(q)$ for critical fluctuations,

$$w(q)=(k_BT\chi_0/V)[1+(A\chi_0)q^2]^{-1}. \quad (32)$$

This power spectrum is approximate and only valid for small q. de Gennes[33] suggests that the accuracy of a power spectrum be tested by the requirement

$$(V/Nk_BC)\textstyle\sum_q w(q)=1. \quad (33)$$

For the spectrum (32) we find near T_c that

$$(V/Nk_BC)\textstyle\sum_q w(q)\cong 0.4, \quad (34)$$

but that (33) is more nearly satisfied at high temperatures. To improve the accuracy of (32) as a probability distribution, we normalize it at every temperature and

[31] M. E. Fisher, in *Proceedings of the International Conference on Magnetism, Nottingham, 1964* (The Institute of Physics and The Physical Society, London, 1965), p. 79.

[32] C. Kittel, *Elementary Statistical Physics* (John Wiley & Sons, Inc., New York, 1958), pp. 133–140.

[33] P. G. de Gennes, in *Magnetism*, edited by H. Suhl and G. Rado (Academic Press Inc., New York, 1963), Vol. III, pp. 115–147.

write $P(q)$ as

$$P(q)=w(q)/\sum w(q)$$
$$=(2\pi)^3(\chi_0 A/Vq_m)[1+(A\chi_0)q^2]^{-1}, \quad (35)$$

where q_m is the wave vector of the zone boundary.

It was argued by Van Hove[9] that for large fluctuations the magnetization decays by spin diffusion leading to a wave-vector–dependent relaxation time

$$\tau(q)=1/\Lambda q^2, \quad (36)$$

with $\Lambda\propto\chi_0^{-1}$. A careful anslysis by Kocinsky[34] shows that the diffusion approximation is a good one but that Λ remains nonzero at T_c. This result is supported by experimental data[35] on Fe but has been disputed by Kawasaki.[36] We have used the experimental values for Λ of Cribier *et al.*[37] which show a slow temperature dependence near T_c.

Using (35) and (36) we can evaluate (30) with the result that

$$\tau_c\cong(a/4\Lambda)(A\chi_0)^{1/2}, \quad (37)$$

where we have taken $q_m=2\pi/a$ and a is the lattice constant. Equation (37) has the observed dependence on χ_0 [cf. (27)] and has the value $\tau_c\cong3\times10^{-14}$ sec at T_c+70°K for $A=2.6\times10^{-12}$ cm^2 and $\Lambda=1.6\times10^{-2}$ cm^2/sec taken from neutron data. This value agrees well with the high-temperature exchange value of 2×10^{-14} sec.

At higher temperatures the power spectrum must be cut off at the exchange frequency, a fact we have not included in the above analysis. If only nearest-neighbor interactions are important, we might expect the fluctuation argument to hold so long as the cluster includes the nearest neighbors of a given spin. At the observed crossover temperature, T_c+66°K, $r_c\cong5$ Å which is about twice the nearest-neighbor separation.

Neutron-diffraction results indicate a slow temperature dependence in Λ and a q^4 term in the fluctuation spectrum.[37] A dominant q^4 term in (35) leads to a $\chi_0^{3/4}$ temperature dependence which is stronger than observed. The decrease of about 25% in Λ observed in the neutron data, results in a slightly steeper slope in Fig. 7. However, Kouvel and Fisher indicate[4] that $\gamma\cong1.25$ in this temperature range and it is likely that the combination $(\chi_0^{1/2}/\Lambda)$ gives a value of γ fortuitously close to $\gamma=1.33$.

Mori[38] has calculated the correlation time for a ferromagnet using a somewhat different approach finding

$$\tau_c\propto(T-T_c)^{-1/3}$$

for $T>1.03T_c$ in disagreement with our results.

D. $T<T_c+30$°K: Ferromagnetic Behavior

Below T_c+30°K the effective exchange frequency becomes constant at 2.8×10^{13} sec^{-1}. One is tempted to take the observed value of $3\omega_d^2\tau_c$ as the full dipolar linewidth, assuming that ω_e has become comparable to ω_d so that the narrowing condition is no longer satisfied.[28] However this would require a change from a Lorentzian to a Gaussian line shape which was not observed. Further ω_d must be much larger than 4.6×10^{12} sec^{-1} in order to fit the high-temperature data. Finally, the transition from extreme narrowing to full dipolar broadening is gradual, with only 70% of the dipolar width occurring at $\omega_d=\omega_e$. Therefore, the change in the temperature dependence of the linewidth at T_c+30°K must be ascribed to other sources.

The most striking feature of the linewidth data below T_c+30°K is its continuity through the Curie temperature. This strongly suggests that the ferromagnetic relaxation mechanism extends into the paramagnetic region. This is not startling since the application of an external field, which is necessary for a spin-resonance experiment, largely destroys the effect of the transition: The magnetization does not go to zero, nor does the susceptibility diverge at T_c. Even in the absence of an external field, however, some properties of the ordered state remain, such as the spin-wave-like peaks which are observed by neutron scattering[39] to 1.15 T_N in MnF_2 and MnO.

The Ornstein-Zernike approximation used in the preceding section cannot be valid in the immediate vicinity of T_c. It predicts that the correlation length and the lifetime of the fluctuations diverge together, giving rise to a magnetization peak at T_c. Careful analysis of the critical region[40] indicates that the approximations of the preceding section are valid only for $(T-T_c)/T_c>1/z$; that is, for $T>T_c+50$°K, where z, the number of nearest neighbors, is 12 in the fcc structure. Thus it is not surprising that a change in behavior is noted near T_c.

It has been suggested[41] that when there is appreciable short-range order in the spin system, it is possible to have highly damped spin-wave-like excitations which scatter neutrons, and in our case, exchange-narrow the resonance line. Such magnons would serve to connect the quasimagnon excitations in the random-phase approximation[40] just below T_c with the Ornstein-Zernike fluctuations just above T_c.

Below T_c, fluctuations in magnetization must be viewed as inhomogeneities in the spatial density of the

---

[34] J. Kocinsky, Acta Phys. Polon. **24**, 273 (1963).
[35] L. Passell, K. Blinowsky, T. Brun, and P. Nielson, Phys. Rev. **139**, A1866 (1965).
[36] K. Kawasaki, Phys. Rev. **145**, 224 (1966); **148**, 375 (1966).
[37] D. Cribier, B. Jacrot, and G. Parette, J. Phys. Soc. Japan **17**, Suppl. BIII, 67 (1962).
[38] H. Mori, Brookhaven National Laboratory Technical Report No. BNL 940 (C-45), 1966 (unpublished).
[39] K. C. Turberfield, A. Okazaki, and R. W. H. Stevenson, Proc. Phys. Soc. (London) **85**, 743 (1965); A. Renninger, S. C. Mass, and B. L. Averbach, Phys. Rev. **147**, 418 (1966).
[40] R. Brout, *Phase Transitions* (W. A. Benjamin, Inc., New York, 1965), p. 43.
[41] W. Marshall, Technical Report, Atomic Energy Research Establishment, Harwell, 1965 (unpublished). Notes prepared by R. W. Lowde, Technical Paper No. 209, Atomic Energy Research Establishment, Harwell, 1966 (unpublished).

quasimagnon gas.[38] The relaxation of fluctuations is therefore governed by the rate at which excess magnons can disappear or diffuse away. These quasimagnons have the same dispersion relation as low-temperature magnons up to a wave-vector-independent temperature factor,[42] which, in the random-phase approximation is found to be simply[40] $M(T)/M(0)$, where $M(T)$ is the magnetization at T. Further, the lifetime of these magnons τ_k is found to be comparable to their frequency.[38]

If we now assume that the magnons giving rise to the density fluctuation are created in numbers proportional to their equilibrium distribution, the net relaxation rate can be written as

$$1/\tau_c \cong \sum_k (1/\tau_k)(n_k/\sum_k n_k), \tag{38}$$

where

$$n_k = (e^{\hbar\omega_k/k_BT}-1)^{-1},$$

and

$$\omega_k = \omega_0 + D(M/M_0)k^2. \tag{39}$$

If we approximate the relaxation rate of the kth magnon by ω_k [cf. Eq. (31), Ref. 38], we can convert the sums in Eq. (38) to integrals which, in the limit $\hbar\omega_{\text{zone boundary}} \gg k_BT$, give

$$(1/\tau_c) = (k_BT/\hbar)(\tfrac{5}{2})\zeta(\tfrac{5}{2})/\zeta(\tfrac{3}{2}) = (1.7T)\times 10^{11}\ \text{sec}^{-1}. \tag{40}$$

The approximation $\hbar\omega_{ZB} > k_BT$ is fairly good for $M/M_0 > 0.1$, which includes the Curie temperature for an 8 kOe applied field. Equation (40) has the value 1×10^{14} sec^{-1} at T_c+30°K which is of the proper order of magnitude. However, (38) leads to an over-all (H/MT^2) temperature dependence of the linewidth, which is in disagreement with Rodbell's results.[16] Obviously this is far too simplified a model for the behavior near the Curie temperature but it does show that an exchange frequency different from zero would exist. Mori[38] has attempted some calculations in the critical region and reported that a minimum in the exchange frequency should occur at $1.03T_c = T_c + 19$°K increasing both above and below this point, while our results indicate that the exchange frequency becomes constant below $1.05T_c$.

V. SPECTROSCOPIC SPLITTING FACTOR

A. Experimental Results

For a thin disk magnetized along its axis, the condition for ferromagnetic resonance is given by

$$\omega_0 = g\mu_B(H_r - N_zM)/\hbar. \tag{41}$$

By measuring the field for resonance H_r as a function of the demagnetizing field $H_d = N_zM$ we can determine the g value from the value of H_r at $H_d = 0$. In Fig. 8 we have plotted the measured values of H_r against values

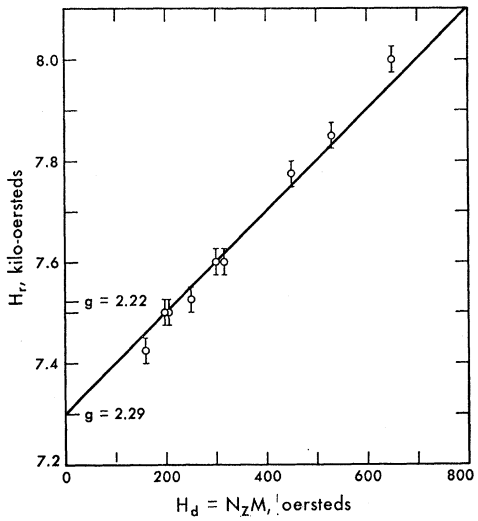

FIG. 8. The field for resonance H_r versus the demagnetizing field H_d. Intercept of a line with slope 1 gives the g value. The point $g=2.22$ gives the position the line would have if the ferromagnetic g value were observed.

of H_d from Ref. 5 for our high-temperature data. The best straight line with a slope of one corresponds to a paramagnetic g value of

$$g_p = 2.29 \pm 0.02. \tag{42}$$

This is higher than values reported in the ferromagnetic region.[14–16]

The resonant field H_r was determined from the position of the maximum in the absorption curves at temperatures for which the expansion in Eqs. (14) and (15) are valid. Near T_c and for several higher temperatures, a two-parameter least-squares fit to the data was made to determine the best values of τ_r and g. This analysis showed that (42) is valid for $T - T_c \gtrsim 10$°K.

The ferromagnetic g value g_f has been measured by several authors[15,16] and found to have the temperature-independent value

$$g_f = 2.22 \pm 0.02, \quad \text{for} \quad T \leq T_c. \tag{43}$$

We have also found this g value at T_c but find a rapid change from the ferromagnetic value (43) to the paramagnetic value (42) at T_c. The temperature dependence of this shift could not be determined from our data.

The measured g shift in Ni,

$$\Delta g_{\text{Ni}} = g_p - g_f = 0.07, \tag{44}$$

is in disagreement with the shift reported by Bagguley and Herrick (BH)[43] in colloidal nickel. They found a shift to the free-electron g value above the Curie point:

$$\Delta g_{\text{BH}} = -0.22. \tag{45}$$

Further, the linewidth was reported to be constant

[42] M. Bloch, Phys. Rev. Letters 9, 286 (1962).

[43] D. M. S. Bagguley and N. J. Harrick, Proc. Phys. Soc. (London) A68, 649 (1954).

above T_c. It is possible, in view of the rapid decline in the amplitude of the signal from nickel, that their signal resulted from a paramagnetic impurity. Preliminary measurements on 100 Å nickel particles in an alumina matrix,[44] using the bimodal cavity, indicate that there is no shift to $g=2.0$ at T_c.

A g shift similar to (44) has been observed at the Curie point of gadolinium single crystals by Rodbell and Moore.[45] This shift, also away from the free-electron value, has the value

$$\Delta g_{\mathrm{Gd}}=-0.06, \tag{46}$$

the negative sign reflecting the fact that the g value of paramagnetic gadolinium is less than $g=2$.

B. g Shifts in Metals

Because the orbital angular momentum is quenched in many paramagnetic salts, g values very near the spin-only value are common. Shifts from $g=2$ result from the mixing of orbital momentum states by the spin-orbit interaction. In metals, the problem is quite different unless the magnetic electrons are highly localized. Even so, the effect of the conduction electrons may be significant. In the iron group metals, for instance, the s-d exchange interaction J_{sd} has been shown[46] to shift the resonance by an amount $\Delta g\approx J_{sd}/E_F$, where E_F is the Fermi energy, in a manner analogous to the Knight shift. In Ni, where $J_{sd}=0.2$ eV,[47] this contribution leads to a g shift of $\Delta g\cong 0.07$. This is of the proper size but it is difficult to account for a 100% change in J_{sd} at T_c.

In conductors large shifts in the g value can result when a small effective mass m^* occurs near a spin-orbit split band edge.[48] The z component of the angular momentum in such cases is of the order $\hbar\Delta/E_g$, where Δ is the spin-orbit splitting and E_g the gap between admixed bands, but the orbital magnetic moment μ_L is of the order $(m/m^*-1)(\Delta/E_g)\mu_B$. This reflects the larger effective radius of gyration resulting from the small effective mass. If we define the g value in terms of the total magnetic moment per electron, we find that

$$|\Delta g|=2\mu_L/\mu_B\cong 2(m/m^*-1)\Delta/E_g, \tag{47}$$

where the sign of the shift must be determined from the details of the band structure.

In order for a g shift (47) to occur near T_c, the band edges involved must pass through the Fermi surface at T_c. In Fig. 9 we show the spin-up band[49,50] in Ni along Λ. Below T_c the Fermi surface lies above the d-band edge L_3. At T_c, this portion of the d band becomes partially emptied so that both up and down spin bands are equally populated. The L_3-L_2' gap E_g is about[50] 0.5 eV and the spin-orbit splitting about 0.07 eV. Using the value $m/m^*=1.5$ obtained from de Haas–van Alphen measurements[51] we obtain a shift

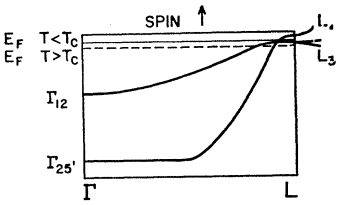

FIG. 9. Schematic spin-up band structure of Ni along Λ (after Ref. 50). The Fermi surface E_F changes position with respect to the band edges as T increases.

$$|\Delta g|\sim 0.1 \tag{48}$$

due to the L_3 band edge. Since at T_c the L_3 edge is no longer occupied, this contribution to the g value disappears. Thus we view the g shift at T_c as a reduction in the orbital magnetic moment resulting from the depopulation of the L_3 d-band neck in the spin-up band at T_c.

Herring has pointed out[52] that the net effect of collective phenomena on the d bands is to make the one-electron approximation a good one. This and the success of the one-electron model in explaining the de Haas–van Alphen data and optical results lead us to believe that the single-electron analysis of the g shift is valid.

VI. HALL EFFECT

In Eqs. (16) and (17) we found that the Hall effect appears as an additional contribution to the absorptive part of the rotation, but is absent from the dispersive part. This makes it possible to separate the Hall effect from the magnetic rotation by fitting the dispersive data to calculated line shapes, and then measuring the deviation of the absorptive data from the calculated values. At most temperatures, no Hall contribution could be detected but from 380 to 420°C the Hall term comprised a measurable part of the absorption signal, although never more than 20%.

Both the magnetic rotation and the Hall angle decrease rapidly with increasing temperature above T_c. The Hall angle has the interesting property of saturating at about 5 kOe above T_c. Therefore, the Hall rotation does not become a significant part of the signal even at high fields. Using standard values of the resistivity and

---

[44] We are indebted to Dr. R. T. Lewis, California Research Corporation, for this sample.

[45] D. S. Rodbell and T. W. Moore, in *Proceedings of the International Conference on Magnetism, Nottingham, 1964* (The Institute of Physics and The Physical Society, London, 1965), p. 227.

[46] D. Shaltiel, J. H. Wernick, H. J. Williams, and M. Peter, Phys. Rev. **135**, A1346 (1964).

[47] J. Mathon and D. Fraitova, Phys. Status Solidi **8**, K37 (1965); **9**, 97 (1965).

[48] C. Kittel, *Quantum Theory of Solids* (John Wiley & Sons, Inc., New York, 1963).

[49] D. C. Tsui and R. W. Stack, Phys. Rev. Letters **17**, 871 (1966).

[50] J. C. Phillips. Phys. Rev. **133**, A1020 (1961); J. C. Phillips and I. F. Matheiss, Phys. Rev. Letters **11**, 556 (1963).

[51] A. S. Josephson and A. C. Thorsen, Phys. Rev. Letters **11**, 554 (1963).

[52] C. Herring, J. Appl. Phys. **37**, 1444 (1966).

TABLE I. Hall angle at H_r.

T (°C)	Magnetic rotation (radians)	Hall angle (radians)	Hall angle Smith[a] (radians)
386.6	16×10^{-3}	-3×10^{-3}	-3.3×10^{-3}
387.3	14	−2.5	
393.6	11	−2.0	−2.2
413.7	4.3	−0.62	−0.66

[a] Reference 53.

Hall constant[53,54] we find that rotations of 10^{-2} to 10^{-5} rad occur between T_c and $T_c+30°$K. In the same temture range, the magnetic rotations vary between 1 and 0.03 rad. Above this temperature, the magnetic rotation decreases less rapidly than the Hall angle, and the Hall angle can be measured over a limited range of temperatures.

At 386.6°C we measure a component of the absorptive rotation which is linear up to 5 kOe and constant beyond with the value 3×10^{-3} rad. This value is determined by measuring θ in Eq. (17) with a precision attenuator and using the value of A determined from the linewidth data. According to Eq. (17) a positive rotation (i.e., in the same sense as the resonant absorption) corresponds to $\theta_H<0$, and, by the definition of the Hall constant, means that the carriers are electrons, as dc data indicate.

Table I shows the Hall angle at the resonant field in the temperature range where it is a significant part of the observed rotation. The values are in good agreement with the dc measurements. This is to be expected, since at this temperature, the relaxation time for carriers is too short to allow them to make a sizeable fraction of an orbit in the applied field during a cycle of the rf field.

Because the Hall data must be extracted with great difficulty from the magnetic data, no attempt has been made to measure carefully the field and temperature dependence. The results indicate that there is no advantage in working at microwave frequencies for Hall measurements, and that the dc values hold at least up to K-band microwave frequencies.

VII. CONCLUSION

We have found that a satisfactory discussion of our results for the magnetic resonance linewidth in nickel above the Curie temperature requires a treatment of the short-range order in the spin system. An application of the Ornstein-Zernike theory for magnetic critical scattering developed by Van Hove was used to predict both the temperature dependence and starting point for the breakdown of exchange-narrowing observed experimentally. The theory was found to hold only above 1.05 T_c which is not surprising, since the model leads to a magnetization peak at T_c. The continuity of the linewidth below 1.05 T_c through the Curie point indicates an extension of ferromagnetic relaxation processes into the paramagnetic region. We have discussed this in terms of the highly damped spin-wave-like excitations thought to exist in the critical region. Using a very rough approximation we find that the exchange-narrowing process does not break down completely; as soon as there is sufficient short-range order, quasimagnons can narrow the line.

In order to account for the abrupt g shift at the Curie temperature we have made use of the band structure of nickel. This would seem to be at variance with the results of the linewidth measurements where the spins were assumed to be localized. However, Kubo *et al.*[55] have shown that the same fluctuation spectrum can be obtained from the itinerate electron model, so that there is no contradiction. As we have no satisfactory explanation of the g shift from the localized d-electron model our results tend to support an itinerate electron picture for nickel.

Note added in proof. A more satisfactory explanation for the g-shift above T_c has been made by Giovanni, *et al.*[56] In this mechanism, the Kittel-Mitchell shift changes sign at T_c due to the details of the conduction electron dynamics.

ACKNOWLEDGMENTS

I am indebted to Professor A. M. Portis, who suggested this problem, for his continued advice and encouragement. It is a pleasure to acknowledge the help of J. Siebert in the construction of the temperature control system and to thank Professor C. Kittel for his valuable suggestions. I am grateful to the National Science Foundation for their support through a Cooperative Graduate Fellowship.

[53] A. W. Smith, Phys. Rev. **30**, 1 (1910).
[54] E. M. Pugh and N. Rostoker, Rev. Mod. Phys. **25**, 151 (1953).
[55] R. Kubo, T. Izuyama, D. T. Kim, and Y. Nagaoka, J. Phys. Soc. Japan **17**, Suppl. BI, 67 (1962).
[56] B. Giovanni, M. Peter, and S. Koide, Phys. Rev. **149**, 251 (1966).